DOI 10.1002/pmic.200700760 *Proteomics* 2008, *8*, 2230–2243

RESEARCH ARTICLE

The up-regulation of 14-3-3 proteins in Smad4 deficient epidermis and hair follicles at catagen

Cunzhong Yuan[1], Liyan Jiao[2]*, Leilei Yang[1], Wantao Ying[2], Zhishang Hu[1, 3], Jinfeng Liu[2], Fang Cui[1], Lei Li[2], Linyi Qian[2], Yan Teng[1], Haiying Hang[3], Xiaohong Qian[2]** and Xiao Yang[1]*

[1] State Key Laboratory of Proteomics, Genetic Laboratory of Development and Diseases, Institute of Biotechnology, Beijing, P. R. China
[2] State Key Laboratory of Proteomics, Beijing Proteome Research Center, Beijing Institute of Radiation Medicine, Changping District, Beijing, P. R. China
[3] Institute of Biophysics, Chinese Academy of Sciences, Beijing, P. R. China

Received: August 2, 2007
Revised: November 23, 2007
Accepted: January 30, 2008

Each postnatal hair follicle (HF) perpetually goes through three phases: anagen, catagen, and telogen. The molecular signals that orchestrate the follicular transition between phases are still largely unknown. Our previous study shows that the keratinocyte specific *Smad4* knockout mice exhibit progressive alopecia due to the mutant HFs failure to undergo programmed regression. To investigate the detailed molecular events controlling this process, the protein profiles of *Smad4* mutant and control epidermal and HF keratinocytes were compared using 2-D difference gel electrophoresis (2-D DIGE) proteomic analysis. Eighty-six differentially expressed protein spots were identified by MALDI-TOF/TOF MS or ESI-MS/MS as 72 proteins, of which 29 proteins were found to be changed during the anagen-catagen transition of HFs in *Smad4* mutants compared with the controls. The differentially expressed proteins represent a wide spectrum of functional classes such as keratin, the cytoskeleton, cellular growth and differentiation, ion combination and transfer, protein enzymes. Notably, we found that the 14-3-3σ protein together with the 14-3-3ζ and 14-3-3β proteins were significantly down-regulated only in wild-type keratinocytes but not in *Smad4* mutant keratinocytes during the catagen phase, suggesting that increased expression of 14-3-3 proteins might contribute to the blockade of catagen initiation in *Smad4* deficient HFs.

Keywords:
2-D DIGE / 14-3-3 proteins / Hair follicle cycling / Keratinocyte

1 Introduction

The postnatal hair follicles (HFs) continually cycle through three phases: organ growth and hair shaft formation (anagen), apoptosis-driven regression (catagen), and relative quiescence (telogen) [1]. During the catagen stage, the HF goes through a highly controlled process of involution that largely reflects a burst of programmed cell death in the majority of follicular keratinocytes [2]. The physiological involution of the HF may be triggered by a variety of stimuli, including signaling *via* death receptors, and by the withdrawal of growth factors that maintain cell proliferation and differentiation in the anagen HF [3]. Before or during catagen, outer root sheath (ORS) keratinocytes produce several important catagen-promoting secreted molecules including fibroblast growth factor-5 short isoform, neurotrophins, transforming growth factor-

Correspondence: Dr. Xiao Yang, Genetic Laboratory of Development and Diseases, Institute of Biotechnology, 20 Dongdajie, Beijing 100071, P. R. China
E-mail: yangx@nic.bmi.ac.cn
Fax: +86-10-63895937

Abbreviations: FABP5, fatty acid binding protein 5; **HF,** hair follicle; **IRS,** inner root sheath; **K5-Cre,** keratin 5-Cre; **ORS,** outer root sheath; **P15,** postnatal day 15; **P20,** postnatal day 20; **PDK1,** 3-phosphoinositide-dependent protein kinase-1; **qRT-PCR,** quantitative real-time PCR; **TGF-β,** transforming growth factor-β

* Both authors contributed equally to this work
** Additional corresponding author: Dr. Xiaohong Qian, E-mail: qianxh1@yahoo.com.cn

β1/2 (TGF-β1/2), insulin growth factor binding protein 3 and thrombospondin-1 [1].

Multiple evidence reveals the important roles of TGF-β signaling during catagen progression [4]. ORS keratinocytes expressing TGF-β receptors become TUNEL positive during catagen [5]. In contrast to corresponding wild-type mice, TGF-β1 knockout mice display significant catagen retardation associated with the decline of apoptotic cells in the regressing ORS [5]. TGF-β2 suppresses proliferation of epithelial cells and triggers the intrinsic caspase network that subsequently terminates anagen in HFs [6, 7]. The up-regulation of TGF-β2 has been shown to mediate all-trans retinoic acid to induce premature HF regression [8]. TGF-β antagonists are effective in preventing catagen-like morphological changes and in promoting elongation of HFs *in vivo* and *in vitro* [9–11]. However, the molecular mechanism underlying the TGF-β triggered apoptosis of follicular keratinocytes is still largely unknown.

TGF-β signals through transmembranous types I and II receptor serine/threonine kinases and intracellular mediators called Smads [12]. The eight identified Smad proteins have been divided into three functional classes: the receptor regulated Smads (Smad1, 2, 3, 5, and 8), the inhibitory Smads (Smad6 and 7), and the common mediator Smad (Smad4) [13]. We and others have previously reported that disruption of *Smad4* in keratinocytes blocks HF regression, resulting in progressive alopecia in mice [14, 15]. During the first anagen phase, *Smad4* mutant follicles appeared to be relatively normal compared with wild-type follicles. During catagen, the *Smad4* mutant follicles were found persisting in an abnormal, anagen-like state. They became further thickened and distorted, and eventually lost their follicular characteristics by the end of the third month in the mutant mice. TUNEL staining revealed that *Smad4* mutants had a decreased number of apoptotic cells in the hair bulb of early catagen HFs [14]. To further investigate the molecular mechanism of Smad4-mediated TGF-β signaling in HF growth and initiation of the catagen phase, we performed 2-D DIGE proteomic analysis of epidermal and HF keratinocytes from the *Smad4* mutant and control mice during anagen and catagen to explore the differentially expressed proteins during the initiation of catagen.

2 Materials and methods

2.1 Genotyping of the keratinocyte specific *Smad4* gene knockout mice

By crossing the keratin 5-Cre (K5-Cre) transgenic mice [16] with the mice carrying conditional *Smad4* alleles [17], we produced the $Smad4^{Co/Co}$;K5-Cre, $Smad4^{Co/+}$;K5-Cre, and wild-type control mice. The offspring were genotyped by PCR analysis [14, 18].

2.2 Preparation of epidermal lysates

Mouse back skin was harvested and subjected to 0.5 M ammonium thiocyanate at 37°C for 55 min with the hypodermis tissue underneath [19]. Epidermal pieces were separated carefully from the dermis, and dissolved in lysis buffer (7 M urea, 2 M thiourea, 4% CHAPS, 65 mM DTT, 0.5% SDS, 5 mM magnesium acetate). Samples were lysed by sonication for a total of 2 min (10 × 6 s pulses at 21% amplitude on ice). After suspending for 1 h at room temperature, the cell lysates were centrifuged twice at 18 000 rpm for 1 h at 4°C. The supernatants were collected by using 2-D Clean-up kit (GE Healthcare) according to the manufacturer's instructions. The proteins were redissolved in buffer (7 M urea, 2 M thiourea, 30 mM Tris, 4% CHAPS) and the concentrations were determined using the modified BioRad Protein Assay as described by the manufacturer.

2.3 2-DE

Protein samples (50 μg) were labeled with 400 pmol of *N*-hydroxysuccinimide cyanine dyes Cy2, Cy3, or Cy5 (GE Healthcare) following the experimental design shown in Fig. 1B and the manufacturer's recommended protocols. The labeling reaction was done at 0°C in the dark for 30 min and the reaction was terminated by addition of 10 nmol lysine at 0°C in the dark for 10 min. Equal volumes of 2 × sample buffer (7 M urea, 2 M thiourea, DTT 4 mg/mL, and 2% Pharmalytes 4–7) were added to the labeled protein samples and the three samples for each gel were mixed according to the experimental design (Fig. 1B). The pooled sample of each gel was diluted with rehydration buffer (7 M urea, 2 M thiourea, 2 mg/mL DTT, and 1% Pharmalytes 4–7) to 450 μL before IEF.

First dimension IEF made use of rehydration loading. IPG strips (240 × 3 × 0.5 mm^3, nonlinear 3–7 pH, GE Healthcare) were rehydrated with CyDye-labeled samples for 12 h at 30 V using the Ettan IPGphor system (GE Healthcare). IEF was performed at maximum current of 50 μA *per* strip and the sequential protocol was done by step and hold at 200 V for 1 h, 500 V for 1 h, 1000 V for 1 h, 8000 V (gradient) for 1 h, and 8000 V for a total of 64 kV·h. The platform temperature was maintained at 20°C. Prior to the second dimension SDS-PAGE, the IPG strips were each equilibrated in 10 mL reducing solution (50 mM Tris pH 8.8, 30% v/v glycerol, 8 M urea, 1% SDS, 1% DTT) with gentle rocking for 15 min to break the disulfide bonds, and then were each rocked in 10 mL alkylating solution (50 mM Tris pH 8.8, 30% v/v glycerol, 8 M urea, 1% SDS, 2.5% w/v iodoacetamide) for 15 min to alkylate the free cysteines. The proteins were further separated on the 12.5% homogeneous SDS-PAGE gels (24 cm × 20 cm × 1 mm) casted with low-fluorescence glass plates utilizing the Ettan Dalt II System (GE Healthcare). The SDS-PAGE gels were run at 15 mA/gel for 30 min and then at 40 mA/gel at 15°C until the bromophenol blue dye edge reached the bottom of the gels. SDS electro-

A

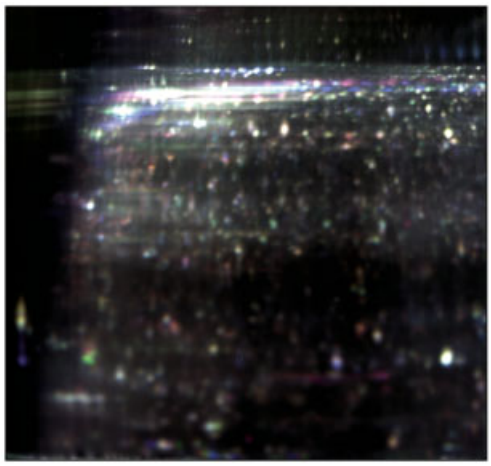

B

Gel	Cy2(blue)	Cy3(green)			Cy5(red)		
		Sample	Genetype	Stage	Sample	Genetype	Stage
A	IS	1	+/+	P15	4	-/-	P15
B	IS	5	-/-	P15	7	+/+	P20
C	IS	8	+/+	P20	10	-/-	P20
D	IS	11	-/-	P20	2	+/+	P15
E	IS	3	+/+	P15	9	+/+	P20
F	IS	6	-/-	P15	12	-/-	P20

Figure 1. 2-D DIGE analysis of *Smad4*$^{+/+}$ and *Smad4*$^{-/-}$ mice epidermis at anagen and catagen. (A) A representative picture of an overlay of three dye scan-images Cy2, Cy3, and Cy5 between samples from *Smad4* mutant and wild-type mice at P20. The green spots represent proteins down-regulated in P20 *Smad4* mutant, whereas red spots represent up-regulated proteins compared to the P20 wild-type control. (B) The experimental design showed individual *Smad4* mutant (−/−) or wild-type (+/+) sample at P15 or P20 was labeled with Cy3 or Cy5. Equal amounts of protein lysates from 12 samples were pooled as the internal standard (IS), and labeled with Cy2.

phoresis running buffer was composed of 25 mM Tris pH 8.8, 192 mM glycine, and 0.1% SDS. For preparative 2-DE gels, 800–1000 μg of proteins were separated by IEF as depicted above, the total VH was 100 kV·h. After the SDS-PAGE separation, the gels were stained by modified colloidal CBB G-250 staining.

CyDye-labeled proteins were visualized using the Typhoon™ 9410 imager (GE Healthcare). The Cy2, Cy3, and Cy5 labeled images were obtained at the excitation/emission values of 488/520 nm BP40, 532/580 nm BP30, 633/670 nm BP30, respectively. All gels were scanned at 200 μm pixel resolution and the maximum pixel intensity *per* scanning channel each gel was ensured between 60 000 and 90 000 pixels by identifying suitable PMT voltage. Region of interest to the gel image was defined and the extraneous areas images were cocropped using ImageQuant™ v5.2 (GE Healthcare). Colloidal CBB stained preparative gels were imaged on ImageScanner (GE Healthcare) at 300 dpi.

2.4 Image analysis

Gel images were analyzed using DeCyder v5.0 software (GE Healthcare). Appropriate number of spots was gained using Batch Processor software before artifacts were removed manually utilizing DeCyder Differential Analysis (DIA) software. Examining the matched results manually one-by-one spot after gel-to-gel automatically matching of the standard spot maps from each gel, succeeded by statistical analysis of protein abundance change between samples, was accomplished using the DeCyder Biological Variation Analysis (BVA) software. Spots in the maps for which the average intensity differed between two appoint groups were selected to be identified by MS.

2.5 In-gel digestion and MS identification

To obtain gel spots of the differentially expressed protein, a preparative gel was run and stained by colloidal CBB in 40% methanol and 10% acetic acid [20]. Gel spots corresponding to proteins differentially expressed were picked out manually. The gel specimens were then destained with 25 mM ammonium bicarbonate/50% ACN. In-gel protein digestion was performed with 12.5 ng/L modified sequencing grade trypsin (Promega) in 25 mM ammonium bicarbonate at 4°C for 40 min prior to overnight at 37°C. The resulting peptides were extracted with 5% TFA at 40°C for 1 h and 2.5% TFA/50% ACN at 30°C for 1 h. The supernatants containing peptides were then collected and vacuum-lyophilized, then analyzed by MALDI-TOF/TOF MS (4700 Proteomics Analyzer, Applied Biosystems, Framingham, MA) or ESI-MS/MS (Q-TOF Micro, Micromass, Manchester, UK). For MALDI MS analysis, the extracts were dissolved in 3 μL of 5 mg/mL CHCA matrix (Sigma, St. Louis, MO) in 0.1% TFA/50% ACN, 0.5 μL of this solution were directly spotted onto the MALDI targets. Internal calibration was used to calibrate the target plate, and six candidate peptides originated from myoglobin (Sigma) digested by trypsin (Promega) were all required to match with a mass accuracy within 10 ppm. Mass of these peptides was well distributed ranging from 700 to 3500 Da, including 748.4352, 941.4727, 1360.7583, 1606.8547, 2601.4915, and 3403.7392. The six most abundant ions present in each spot were selected to run MS/MS (with the excluding of trypsin autolytic peptides 1045.577 and 2211.104 Da). Peptide spectra were acquired under positive ion and reflection mode with a mass range from 900 to 2500 Da. The values of laser energy were set at 5000 for MS and 6000 for MS/MS. Total spectra *per* spot were set at 1000 for MS and 2500 for MS/MS. For ESI-MS/MS analysis, lyophilized peptide mixtures were dissolved with 5.5 μL of 0.1% formic acid in 2% ACN and injected by autosampler onto a 0.3×1 mm^2 trapping column (PepMap C18, LC Packings) using a CapLC system. Peptides were directly eluted into Q-TOF Micro at 200 nL/min on a C18 column (75 μm × 15 cm, LC Packings) with a gradient of 4–95% solvent B (80% ACN/20% water) in A (2% ACN/0.1% formic

acid/98% water) for 65 min: 4–30% solvent B in 35 min, 30–95% B in 9.5 min, 95% B for 5 min, 95–4% B in 2 min, and then 4% B for 9 min. The capillary voltage was set at 3000 V. Acquisition of mass ranged from 400 to 1500 Da for MS and 100 to 2000 Da for MS/MS. MS acquisition time was set at 10–50 min.

2.6 Database searching

The raw MALDI-TOF/TOF spectra were processed using Data Explorer software (Version 4.0, Applied Biosystems) with the following settings: Peak filtering for MS was from 900 to 2500 Da with a 20 S/N ratio, a peak density of 50 peaks/200 Da, a maximum of 65 peaks/spot, and the mass of 1045.577, 2211.104, 2225.175, 2230.234, 2283.230, and 2297.215 were put into the MS exclusion list with a tolerance of 50 ppm; peak filtering for MS/MS was from 60 to 20 Da below each precursor mass with a minimum S/N filter of 15, a peak density of 50 peaks/200 Da. Subsequently the mass lists were searched against the NCBInr protein database (November 5, 2005, 3 021 705 sequences) with taxonomy of *Mus musculus* (96 605 sequences) using a local MASCOT search tool (Version 1.9) under combined mode (MS plus MS/MS) with following parameters: trypsin specificity, one missed cleavage, cysteine carbamidomethylation and methionine oxidation as variable modifications, the peptide tolerance at 0.2 Da, and the MS/MS tolerance at 0.25 Da. After the Q-TOF analysis, the pick list files were generated with MassLynx3.5 (Micromass) (smooth 3/2 Savitzky Golay and center 4 channels/80% centroid) and used to search against the NCBInr protein database (November 5, 2005, 3 021 705 sequences) with taxonomy of *M. musculus* (96 605 sequences) by the local MASCOT search engine with the same parameters for MALDI-TOF/TOF data. An identification was considered to be positive only if its MOWSE score surpassed the threshold value for 95% confidence level (62 for MALDI-TOF/TOF data, 35 for Q-TOF data) in MASCOT. For those protein with only one peptide matched (Supporting Information Table S1), the MS/MS spectrum was carefully inspected to assure fidelity (Supporting Information Fig. S1). To remove redundancy due to the assignment multiprotein group, only the first default matching for each protein group was retained except that when the first default matching was an unnamed product, a protein with clearly annotated name would be retained.

2.7 Cluster analysis

A two-way hierarchical cluster analysis of the normal volume ratios of differential expressed proteins was performed, with correlation (uncentered) and complete linkage method for the calculation of the distance by Cluster v 3.0 (Stanford University). For *k*-means clustering, the *k*-means algorithm partitioned the genes into *k* discrete clusters on the basis of their expression. The number *k* (50) was preselected.

2.8 Western blot and immunofluorescence

Proteins (20 μg) were electrophoresed on 12% SDS-PAGE and transferred onto PVDF (Millipore) on a Mini Trans-Blot Cell (BioRad). Immunoblotting was performed using the following antibodies: 14-3-3σ (Santa Cruz), HSP27 (Santa Cruz), β-tubulin (Santa Cruz). Membrane was visualized with an ECL kit (Cell Signaling). Immunofluorescene staining was performed on 9 μm frozen sections of back skin embedded in Cryomatrix (Therm). Frozen sections were fixed in 4% paraformaldehyde. Primary antibody was goat anti-14-3-3σ (Santa Cruz), and antigens were visualized with FITC-conjugated secondary antibodies (ZYMED).

2.9 RNA isolation, real time (RT)-PCR, and quantitative RT-PCR (qRT-PCR)

Epidermis was separated from the dermis as described [21]. Total RNAs were isolated from epidermis using TRIzol reagent (Invitrogen) based on the suggested protocol. RT-PCR analyses were done by using the mRNA Selective PCR kit (TaKaRa). qRT-PCR was preformed by BioRad MyiQ Optical System 2.0. Primers used to amplify the genes were listed below: 14-3-3β, 5′-TCTTCCTGGC GTGTCATCTCC-3′ and 5′-CACTTTGCTTTCTGCCTGGGT-3′; 14-3-3ζ, 5′-GTT GTAGGAGCCCGTAGGTCA-3′ and 5′-GGCCAAGTAAC-GGTAGTAGTCAC-3′; fatty acid binding protein 5 (FABP5), 5′-GGAAGGAGAGCACGATAAC-3′ and 5′-CCAGGATG-ACGAGGAAG-3′; enolase 1, 5′-TCCTGGAGAACAAAGA-AGC AC-3′, and 5′-TTGCCAGACCTGTAGAACTCG-3′; β-actin primers (5′-GTAAAGA CCTCTATGCCAACA-3′ and 5′-GGACTCATCGTACTCCTGCT -3′) were used as the internal control.

3 Results

3.1 Differential protein expression between *Smad4* deficient and control epidermis during the catagen phase

Protein lysates of the epidermis from three wild-type mice ($Smad4^{+/+}$) were compared with that from three littermate $Smad4^{Co/Co}$;K5-Cre ($Smad4^{-/-}$) mice at postnatal day 15 (P15, anagen) and postnatal day 20 (P20, catagen) utilizing 2-D DIGE (Figs. 1A and B). Each sample was labeled with Cy3 or Cy5, respectively, as shown in Fig. 1B. Protein expression changes were identified using the Batch Processor software. The estimated number of protein spots was set at 1600 in the pH range of 3–7. The rate of match was improved to 87.68 ± 1.14% after manual adjustment. Only spots with a 1.2-fold change and $p<0.05$ that were present in all analytical gels were considered significant. Comparing P15 *Smad4* mutants ($Smad4^{-/-}$) to controls ($Smad4^{+/+}$), the number of identified proteins from 24 spots with a decrease or increase in expression level was 13 and 11, respectively. Compared to

P20 *Smad4*$^{+/+}$ controls, 52 protein spots showed significant up-regulation and 35 spots showed significant down-regulation in the P20 *Smad4*$^{-/-}$ epidermis. We found that 204 protein spots were differentially expressed between P15 and P20 wild-type HFs (with a two-fold change and $p<0.05$). These protein spots should contain the key proteins that are involved with regulating the anagen–catagen transition in wild-type HFs. About 186 differentially expressed protein spots were detected between P15 and P20 *Smad4* mutant HFs (with a two-fold change and $p<0.05$).

Altogether, 131 differentially expressed proteins that could be visualized with colloidal CBB staining were excised from the 2-D gels and identified by MALDI-TOF/TOF or ESI-MS/MS followed by database interpretation. Eighty-six protein spots were positively identified as 72 proteins and are listed in Table 1 and Table 2, Supporting Information Table S1 and Fig. S1. These differentially expressed proteins are involved in various biological functions including the cytoskeleton, growth and differentiation, ion combination and transfer, protein enzymes, *etc.* (Fig. 2A).

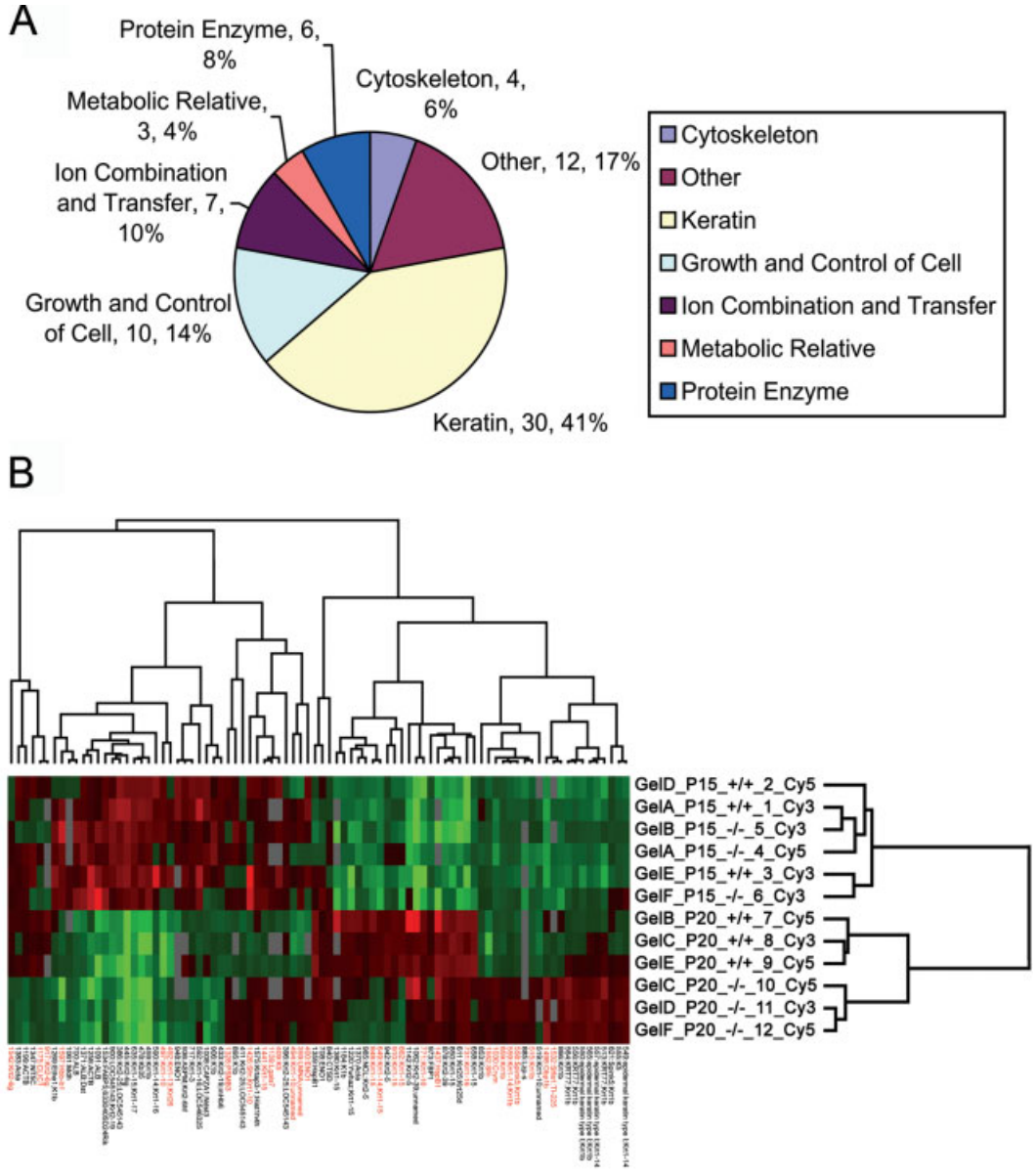

Figure 2. Clustering analysis of differentially regulated proteins in *Smad4* mutant epidermis. (A) Pie chart showing the functions of the 72 differentially expressed proteins in *Smad4* mutant epidermis *versus* wild-type epidermis. (B) Hierarchical clustering analysis of proteins differentially expressed in *Smad4*$^{+/+}$ and *Smad4*$^{-/-}$ epidermis. Proteins up-regulated were in red and down-regulated in green. The degree of color saturation corresponds with the ratio of gene expression shown at the bottom of the image. The names of 29 proteins whose expression was changed during the transition of HFs in *Smad4* mutants compared with the controls were marked in red.

Table 1. Proteins identified by MALDI-TOF/TOF MS

Classification	Master no.	Accession	Protein name	Matched peptides (unmatched peptides)	MS/MS	Sequence coverage (%)	MOWSE score	Fold change			
								$P15^{-/-}/P15^{+/+}$	$P20^{-/-}/P20^{+/+}$	$P20^{+/+}/P15^{+/+}$	$P20^{-/-}/P15^{-/-}$
Keratin	386	gi|51092291	Keratin complex 2, basic, gene 25	17 (48)	3	26	140	−1.39			
Keratin	386	gi|63671930	Predicted: similar to type II keratin Kb23	13 (52)	3	21	105	−1.39			
Keratin	396	gi|51092291	Keratin complex 2, basic, gene 25	20 (46)	5	34	253		1.26		
Keratin	396	gi|63671930	Predicted: similar to type II keratin Kb23	14 (51)	5	26	209		1.26		
Keratin	409	gi|16303309	Type II keratin 5	18 (47)	1	30	107		1.42	−2.44	−1.19
Keratin	411	gi|63680623	Keratin complex 2, basic, gene 25	19 (47)	5	29	70	1.28			
Keratin	411	gi|63671930	Predicted: similar to type II keratin Kb23	14 (52)	5	27	68	1.28			
Keratin	433	gi|11321332	Type II hair keratin	17 (48)	6	40	284	−1.22			
Keratin	433	gi|1903238	Type II intermediate filament of hair keratin	20 (45)	7	43	326	−1.22			
Keratin	478	gi|47523977	Keratin complex 2, basic, gene 35	18 (47)	4	33	143	−1.42			
Keratin	494	gi|125069	Keratin, type I cytoskeletal 10 (cytokeratin 10) (56 kDa cytokeratin) (keratin, type I cytoskeletal)	18 (47)	5	34	336		1.89		
Other	494	gi|26349495	Unnamed protein product	19 (46)	5	46	360		1.89		
Keratin	513	gi|66774007	Keratin, type II cytoskeletal 1b	10 (55)	2	18	89		1.63		
Keratin	513	gi|57113771	TPA: embryonic type II keratin 1; K1-emb	25 (40)	7	53	481		1.63		
Keratin	515	gi|38565071	Keratin 1b	14 (51)	2	60	167		1.54		
Keratin	515	gi|57113771	TPA: embryonic type II keratin 1; K1-emb	22 (43)	6	45	575		1.54		
Keratin	519	gi|7638398	Epidermal keratin 10	17 (48)	4	52	369		1.65		
Other	519	gi|26345440	Unnamed protein product	25 (40)	6	49	514		1.65		
Keratin	549	gi|387398	Epidermal keratin type I	14 (51)	–	34	89		1.48		
Keratin	549	gi|21489935	Keratin complex 1, acidic, gene 14	16 (49)	–	30	92		1.48		
Keratin	555	gi|16303309	Type II keratin 5	17 (48)	1	29	84		1.5		
Keratin	556	gi|66774007	Keratin, type II cytoskeletal 1b	10 (55)	2	15	107		1.6		
Keratin	556	gi|57113771	TPA: embryonic type II keratin 1; K1-emb	21 (44)	6	44	519		1.6		
Keratin	557	gi|387398	Epidermal keratin type I	20 (45)	4	51	237	1.44	1.61		
Keratin	557	gi|21489935	Keratin complex 1, acidic, gene 14	25 (40)	4	52	262	1.44	1.61		
Protein enzyme	558	gi|57282595	Spink5 protein	25 (40)	–	19	84	1.44	1.61		
Keratin	558	gi|57113771	TPA: embryonic type II keratin 1; K1-emb	12 (53)	3	26	91	1.44	1.61		
Keratin	559	gi|21489935	Keratin complex 1, acidic, gene 14	16 (49)	–	37	84		1.35		
Keratin	559	gi|57113771	TPA: embryonic type II keratin 1; K1-emb	11 (54)	4	27	221		1.35		
Keratin	564	gi|66774007	Keratin, type II cytoskeletal 1b	10 (55)	2	18	100		1.68		
Keratin	564	gi|57113771	TPA: embryonic type II keratin 1; K1-emb	22 (43)	6	51	503		1.68		
Keratin	590	gi|21489935	Keratin complex 1, acidic, gene 14	14 (51)	1	30	113			−3.33	−1.77
Keratin	590	gi|6680604	Keratin complex 1, acidic, gene 16	17 (49)	4	28	217			−3.33	−1.77
Keratin	592	gi|6680604	Keratin complex 1, acidic, gene 16	14 (50)	1	28	81			−2.84	−1.74
Other	592	gi|63746523	Predicted: similar to UBE-1C2 protein	17 (48)	–	22	74			−2.84	−1.74
Keratin	611	gi|19526922	Keratin 25A	13 (52)	1	24	87		−1.31		
Keratin	611	gi|51766423	Keratin 25D	15 (50)	5	28	185		−1.31		
Keratin	649	gi|21489935	Keratin complex 1, acidic, gene 14	8 (57)	2	14	83		−1.69	2.75	1.54
Keratin	649	gi|6680602	Keratin complex 1, acidic, gene 15	15 (50)	5	33	175		−1.69	2.75	1.54
Keratin	658	gi|34784398	Krt1-15 protein	16 (49)	4	34	191		−1.81	2.94	1.66
Ion combination and transfer	700	gi|164318	Albumin	14 (51)	3	24	84	1.59			
Ion combination and transfer	700	gi|33859506	Albumin 1	15 (50)	3	30	92	1.59			
Keratin	771	gi|6680604	Keratin complex 1, acidic, gene 16	14 (51)	2	26	121			5.08	2.85
Protein enzyme	821	gi|28524303	Predicted: serine protease inhibitor, Kazal type 5 (*M. musculus*)	21 (44)	–	16	74		1.21		
Keratin	821	gi|57113771	TPA: embryonic type II keratin 1; K1-emb	14 (51)	4	27	102		1.21		

Table 1. Continued

Classification	Master no.	Accession	Protein name	Matched peptides (unmatched peptides)	MS/MS	Sequence coverage (%)	MOWSE score	Fold change			
								$P15^{-/-}/P15^{+/+}$	$P20^{-/-}/P20^{+/+}$	$P20^{+/+}/P15^{+/+}$	$P20^{-/-}/P15^{-/-}$
Protein enzyme	840	gi|6753556	Cathepsin D	7 (58)	2	20	74	1.2	1.27		
Protein enzyme	840	gi|18043133	Ctsd protein	6 (59)	2	41	83	1.2	1.27		
Keratin	848	gi|6680602	Keratin complex 1, acidic, gene 15	14 (51)	2	27	106		−1.8	3.05	1.4
Keratin	848	gi|34784398	Krt1-15 protein	14 (51)	2	27	106		−1.8	3.05	1.4
Keratin	850	gi|34784398	Krt1-15 protein	17 (48)	5	32	184		−1.66	4.77	2.16
Keratin	866	gi|38565071	Keratin 1b	13 (52)	3	68	177		1.69	1.6	2.76
Keratin	866	gi|57113771	TPA: embryonic type II keratin 1; K1-emb	16 (49)	4	33	209		1.69	1.6	2.76
Keratin	900	gi|63671930	Predicted: similar to type II keratin Kb23	24 (41)	4	39	163		1.29		
Keratin	900	gi|11321332	Type II hair keratin	21 (44)	3	47	151		1.29		
Growth and control of cell	936	gi|60391791	Abnormal spindle-like microcephaly-associated protein homolog	39 (26)	–	9	75	−1.34			
Keratin	936	gi|29789317	Keratinocyte associated protein 1	16 (49)	3	28	135	−1.34			
Growth and control of cell	1359	gi|424145	HSP27	7 (58)	3	34	157		−1.4		
Growth and control of cell	1359	gi|91319	Stress protein, 25K	7 (58)	3	33	155		−1.4		
Ion combination and transfer	1371	gi|26986064	Albumin	9 (56)	3	47	119	1.48	−1.5	−2.15	−4.69
Ion combination and transfer	1371	gi|19745146	Dystonin isoform e	37 (28)	–	12	108	1.48	−1.5	−2.15	−4.69
Growth and control of cell	1534	gi|6754450	FABP5, epidermal	11 (54)	3	57	137		1.71		
Other	1534	gi|63492265	Predicted: hypothetical protein LOC70715	3 (62)	2	8	88		1.71		

A hierarchical clustering analysis of the positively identified 86 protein spots whose expression varied in the 12 samples tested is shown in Fig. 2B. In the dendrogram, samples from P15 (anagen) were initially separated from P20 (catagen), demonstrating the great discrepancy in protein expression patterns between the epidermis during anagen and catagen. Samples from $Smad4^{+/+}$ and $Smad4^{-/-}$ mice at P15 were grouped in a tight cluster away from the others, indicating the similarity in their protein expression patterns. This is consistent with our previous studies showing that there were no obvious phenotypes observed in $Smad4^{-/-}$ HFs at P15 compared with their littermate controls. Samples from $Smad4^{+/+}$ and $Smad4^{-/-}$ mice at P20 were clustered next to each other, and there were some obvious differences in their expression patterns. Notably, 29 proteins were changed during the HF anagen–catagen transition in *Smad4* mutants compared with the controls (Fig. 2B, names in red).

3.2 Expression of keratins was significantly altered in *Smad4* mutants

Keratins are major structural proteins in skin epithelial cells, and tightly regulated in a manner specific to the differentiation stage [22]. Figure 3A shows cropped 2-D gel images of a selected number of keratins that were identified as being differentially expressed between the epidermis of $Smad4^{+/+}$ and $Smad4^{-/-}$ mice. Graphic comparisons of the pixel volume ratio of these selected proteins are shown in the following graph (right panel in Fig. 3A). Keratins 1 and 10, markers of the suprabasal epidermis and the inner root sheath (IRS), were expressed at a comparable level between the $Smad4^{+/+}$ and $Smad4^{-/-}$ mice at P15. In $Smad4^{+/+}$ mice at P20, there was a dramatic decline in the expression of keratins 1 and 10, but in $Smad4^{-/-}$ mice, their expression persisted at a relatively high level. The expression pattern of keratin 6, an early differentiation marker of keratinocyte, was similar to that of keratins 1 and 10. Keratins 5 and 14, which are usually restricted to the proliferating basal layer of the epithelium and the ORS, were expressed at higher levels in *Smad4* mutants than $Smad4^{+/+}$ control mice at P20. Keratin 15, an epithelial stem cell marker, was expressed at a relatively lower level in both wild-type and *Smad4* mutant mice at P15. The expression of keratin 15 was significantly upregulated in the wild-type epidermis but not in the *Smad4* mutant epidermis at P20.

Table 2. Proteins identified by ESI-MS/MS

Classification	Master no.	Accession	Protein name	Matched peptides	Sequence coverage (%)	MOWSE score	Fold change			
							$P15^{-/-}/P15^{+/+}$	$P20^{-/-}/P20^{+/+}$	$P20^{+/+}/P15^{+/+}$	$P20^{-/-}/P15^{-/-}$
Cytoskeleton	359	gi|220474	Lamin A	1	2	57		2.03		
Other	359	gi|12859782	Unnamed protein product	3	6	155		2.03		
Growth and control of cell	400	gi|13278412	Eno1 protein	1	3	38	−1.75		−2.22	1.35
Keratin	445	gi|9910294	Keratin complex 2, basic, gene 6 g	2	4	120		1.21	−10.67	−7.24
Keratin	459	gi|38565071	Keratin 1b	1	5	81			−5.01	−8.04
Keratin	492	gi|52783	47 kDa keratin	1	3	78		−1.79	3.04	1.17
Keratin	492	gi|85701899	Keratin 25B	1	1	60		−1.79	3.04	1.17
Keratin	497	gi|387397	Epidermal keratin subunit I	1	2	91			−5.1	2.39
Keratin	550	gi|387398	Epidermal keratin type I	2	6	143	1.38	1.45		
Keratin	550	gi|38565071	Keratin 1b	1	5	65	1.38	1.45		
Keratin	565	gi|387398	Epidermal keratin type I	5	19	233	1.28	1.48		
Keratin	565	gi|38565071	Keratin 1b	1	5	81	1.28	1.48		
Keratin	635	gi|741022	Keratin 15	1	2	75		−1.24		
Keratin	635	gi|7106335	Keratin complex 1, acidic, gene 17	1	3	43		−1.24		
Keratin	662	gi|6680602	Keratin complex 1, acidic, gene 15	7	21	368		−2.22	2.4	1.07
Growth and control of cell	708	gi|12963491	Enolase 1, alpha nonneuron	1	2	57		1.33		
Keratin	717	gi|82936608	Predicted: similar to type I hair keratin KA28	5	15	313		−1.45		
Keratin	731	gi|11559579	Keratin intermediate filament 16a	2	4	92	2.2		9.05	3.46
Keratin	853	gi|38565071	Keratin 1b	1	5	81		1.39		
Keratin	859	gi|38565071	Keratin 1b	1	5	81		1.36		
Keratin	878	gi|51092293	Keratin complex 2, basic, gene 39	6	14	338		−1.35		
Protein Enzyme	885	gi|7305247	P lysozyme structural	1	8	53				2.75
Keratin	895	gi|38565071	Keratin 1b	1	5	88		1.27		
Keratin	906	gi|38565071	Keratin 1b	2	9	123		−1.6	−1.32	−2.82
Keratin	910	gi|741022	Keratin 15	1	2	79			2.01	1.13
Keratin	917	gi|9910294	Keratin complex 2, basic, gene 6g	1	3	77		−1.85		
Keratin	942	gi|16303309	Type II keratin 5	2	3	84		−1.44		
Growth and control of cell	948	gi|13278412	Eno1 protein	1	3	70	−1.52			
Metabolic relative	973	gi|6688689	Liver fructose-1,6-bisphosphatase	2	7	140	−1.3			
Other	985	gi|53454	Nucleolin	2	3	156			2.15	1.42
Keratin	985	gi|16303309	Type II keratin 5	1	2	69			2.15	1.42
Cytoskeleton	1008	gi|595917	Capping protein alpha 1 subunit	5	25	261			−1.8	−2.28
Other	1008	gi|11385420	Heparan sulfate *N*-deacetylase/*N*-sulfotransferase 3	1	1	45			−1.8	−2.28
Growth and control of cell	1030	gi|7710012	Crystallin, mu	3	12	206		1.55	1.23	2.23
Metabolic relative	1061	gi|319837	Malate dehydrogenase (EC 1.1.1.37), cytosolic	1	3	81		−1.2		
Keratin	1062	gi|51092293	Keratin complex 2, basic, gene 39	8	17	510			10.31	7.8
Other	1062	gi|26324736	Unnamed protein product	1	2	43			10.31	7.8
Ion combination and transfer	1091	gi|19353306	Albumin 1	3	5	151			−3.67	−8.08
Growth and control of cell	1139	gi|3913978	Galectin-7	1	8	74		1.36		
Keratin	1142	gi|16303309	Type II keratin 5	2	4	77			4.98	2.72
Ion combination and transfer	1175	gi|13435562	Chloride intracellular channel 1	3	13	159		−1.3		
Cytoskeleton	1175	gi|49868	Put. β-actin (aa 27–375)	1	5	39		−1.3		
Keratin	1184	gi|38565071	Keratin 1b	1	4	54			2.51	1.41

Table 2. Continued

Classification	Master no.	Accession	Protein name	Matched peptides	Sequence coverage (%)	MOWSE score	Fold change			
							$P15^{-/-}/P15^{+/+}$	$P20^{-/-}/P20^{+/+}$	$P20^{+/+}/P15^{+/+}$	$P20^{-/-}/P15^{-/-}$
Cytoskeleton	1199	gi|49868	Put. β-actin (aa 27–375)	2	6.67	110		−1.7		
Growth and control of cell	1220	gi|1526539	14-3-3 zeta	2	10	138		−1.7		
Keratin	1220	gi|6680602	Keratin complex 1, acidic, gene 15	5	14	356		−1.7		
Cytoskeleton	1258	gi|49868	Put. β-actin (aa 27–375)	4	18	153			−2.75	−3.98
Growth and control of cell	1269	gi|12963539	ETHE1 protein	1	5	83			−1.49	−2.02
Keratin	1269	gi|38565071	Keratin 1b	1	4	53			−1.49	−2.02
Protein enzyme	1328	gi|68085773	Proteasome beta 3 subunit	4	18	132	1.35			
Metabolic relative	1347	gi|7657031	5′,3′-Nucleotidase, cytosolic5′,3′	3	22	121		−1.4		
Cytoskeleton	1370	gi|49864	α-Actin (aa 40–375)	1	4	87		−1.6		
Keratin	1380	gi|6680602	Keratin complex 1, acidic, gene 15	4	6	193	−1.66			
Cytoskeleton	1383	gi|49864	α-Actin (aa 40–375)	1	4	111		−1.4		
Growth and control of cell	1426	gi|7106546	14-3-3 protein sigma	2	8	92		1.36		
Keratin	1426	gi|387397	Epidermal keratin subunit I	1	2	101		1.36		
Other	1437	gi|424145	HSP27	1	5	49			4.68	10.99
Keratin	1441	gi|741022	Keratin 15	1	2	112		1.37		
Other	1498	gi|1835145	Odorant binding protein Ib	1	10	89		2.04		
Other	1532	gi|47679086	Stefin A1	2	21	65		1.41	1.35	2.03
Other	1532	gi|1167510	TI-225	1	12	62		1.41	1.35	2.03
Protein enzyme	1542	gi|6753556	Cathepsin D	1	2	42		−1.23		
Growth and control of cell	1552	gi|7106546	14-3-3 protein sigma	1	4	51		2.5		
Keratin	1575	gi|1944401	High-sulfur keratin protein	1	17	50		1.5		
Other	1575	gi|37590121	Hist1h4h protein	2	16	95		1.5		
Ion combination and transfer	1597	gi|1183932	Hemoglobin beta-1 chain	2	14	119			−1.91	−4.81

Western blot analysis confirmed that keratin 1 was down-regulated in wild-type mice but not in *Smad4* mutants at P20 (Fig. 3B). Semiquantitative RT-PCR analysis showed that there was an obvious decline of keratin 15 expression in *Smad4* mutant mice at both P20 and P42 (*i.e.*, during the second catagen) compared with wild-type controls (Fig. 3C).

3.3 Disruption of *Smad4* resulted in aberrant expression of proteins involved in cell proliferation, differentiation, and apoptosis

Figure 4A shows a number of proteins that were differentially expressed between the epidermis of $Smad4^{+/+}$ and $Smad4^{-/-}$ mice. These proteins are involved in cell proliferation, differentiation and apoptosis. Graphic comparisons of the pixel volume ratio of these selected proteins are shown on the right (Fig. 4A). Cathepsin D and enolase 1 were expressed at a comparable level in the *Smad4* mutants at P15, but were significantly up-regulated in *Smad4* mutant mice at P20 compared with wild-type mice at the same age (Fig. 4A). These were confirmed by qRT-PCR (Fig. 4B) and RT-PCR (Fig. 4C). Galectin7, FABP5, and 14-3-3σ were down-regulated in wild-type but not *Smad4* mutant mice at P20, while their expression level was equivalent in *Smad4* mutants and controls at P15 (Fig. 4A). Heat shock protein 27 (HSP27) was down-regulated in *Smad4* mutants at both P15 and P20 (Fig. 4A). The expression of FABP5 (Figs. 4C and D) and HSP27 (Fig. 4E) was verified by qRT-PCR, RT-PCR, or Western blot.

3.4 14-3-3 proteins failed to be down-regulated in the epidermis of *Smad4* mutant mice during catagen

The expression of 14-3-3σ in the epidermis and HFs of *Smad4* mutant and control mice during both anagen and catagen was validated by immunofluorescence (Figs. 5A–H). The results showed that 14-3-3σ was expressed at a comparable level in the suprabasal epidermis and the IRS of HFs in wild-type (Figs. 5A and C) and *Smad4* mutant mice (Figs. 5B and D) at P15. At P20, the expression of 14-3-3σ was drama-

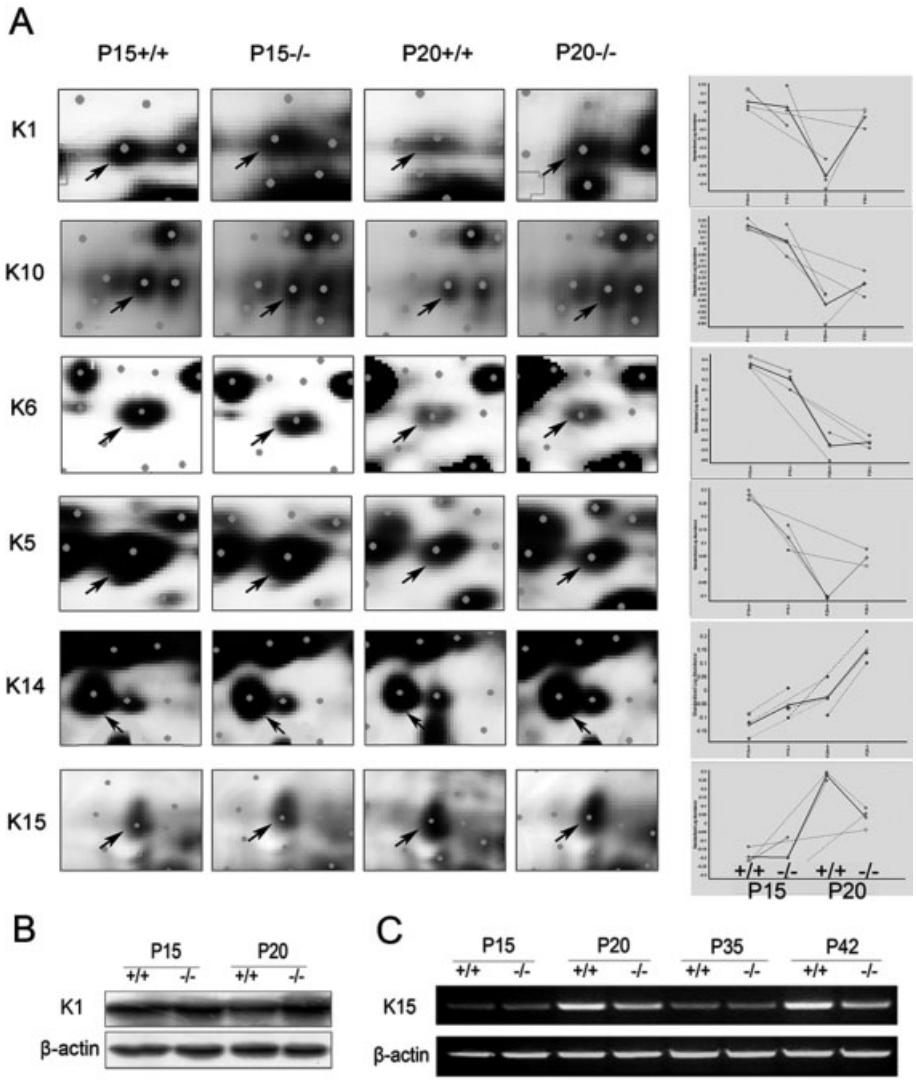

Figure 3. Differentially expressed keratins in *Smad4* mutants. (A) Cropped 2-D gel images of keratins of *Smad4*$^{+/+}$ and *Smad4*$^{-/-}$ epidermis at P15 and P20. Graphic comparisons of pixel volume ratio of these selected proteins were shown on the right. (B) Western blot analysis of keratin 1. (C) RT-PCR analysis of keratin 15.

tically decreased in both the suprabasal epidermis (Fig. 5E) and the IRS (Fig. 5G) of wild-type mice. However, expression of 14-3-3σ persisted at a relatively high level in the *Smad4* mutant mice (Figs. 5F and H). The Western blot data were consistent with the differences observed by the proteomics analysis (Fig. 5I). Real-time PCR revealed that the other two members of the 14-3-3 protein family, 14-3-3ζ and 14-3-3β, were also down-regulated in the wild-type epidermis at P20 but not in the *Smad4* mutant epidermis at the same age (Figs. 5J and K).

4 Discussion

Our previous studies show that targeted disruption of *Smad4* in the epidermis results in progressive hair loss due to defective postnatal HF cycling and early onset of neoplasia in the skin [14]. In this study, we applied DIGE-based proteomics to study the *Smad4*-mediated TGF-β signals in that controlling of HF regression. Twelve epidermal samples, obtained from *Smad4* mutant and littermate control mice at during anagen or catagen, were labeled with different fluorophores. The samples and were run in on six gels, thereby minimizing the technical variation that has been reported to be as high as 20–30% [23]. This enabled us to quantitate real biological differences with high sensitivity, covering epidermal proteomes and the investigation of their dynamic changes throughout the onset of catagen after loss of *Smad4* in keratinocytes.

In wild-type HFs, 204 protein spots were differentially expressed between P15 and P20, suggesting that these proteins might play key roles during the transition of HFs from anagen to catagen. Among them, 29 proteins were changed between P15 and P20 *Smad4* mutants, indicating that these differentially regulated proteins might be involved in the defective programmed regression of HFs in *Smad4* mutants.

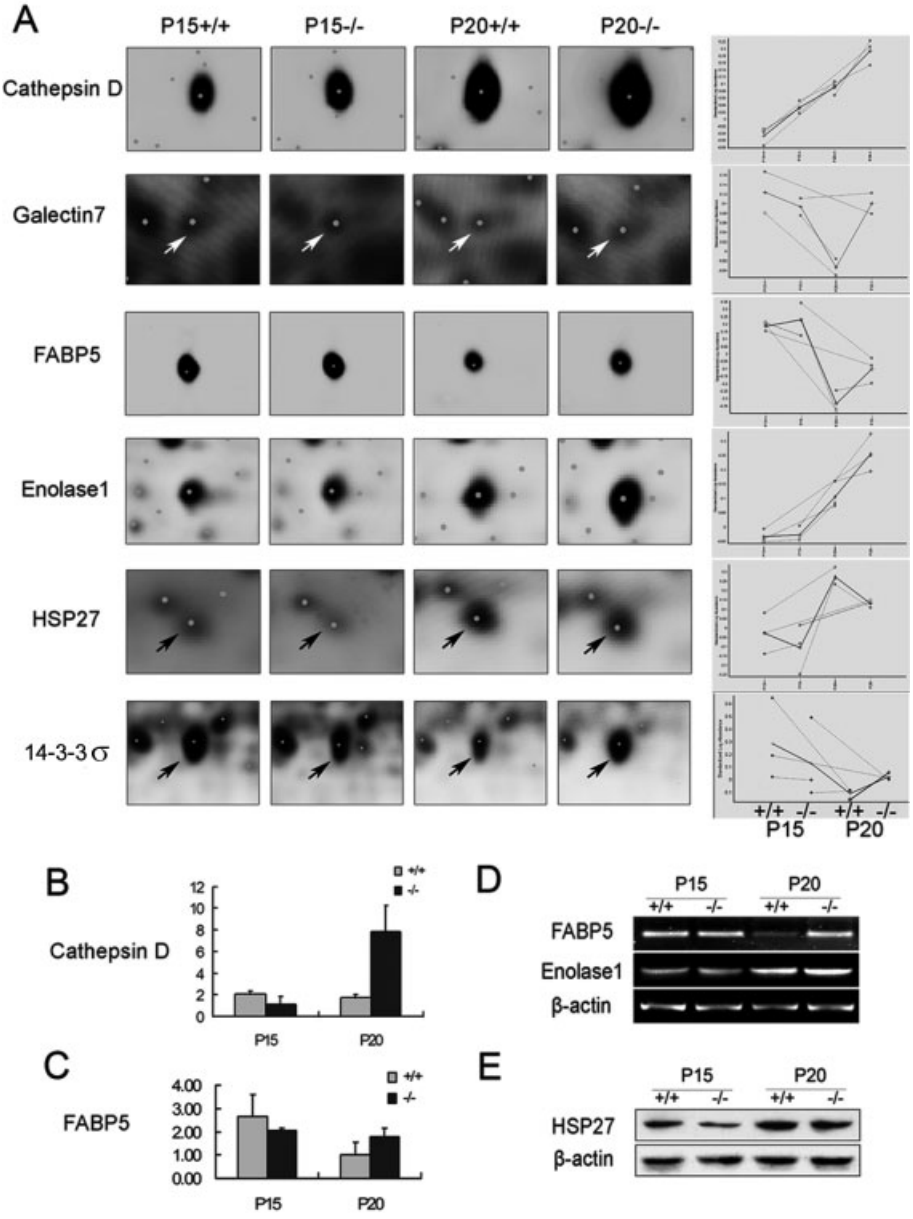

Figure 4. Validation of differentially expressed proteins involved in cell proliferation, differentiation, and apoptosis in *Smad4* mutant epidermis. (A) Expanded region of differentially expressed protein spots of *Smad4*$^{+/+}$ and *Smad4*$^{-/-}$ epidermis at P15 and P20. Graphic comparisons of pixel volume ratio of these selected proteins were shown on the right. (B–C) qRT-PCR analyses of cathepsin D (B) and FABP5 (C). (D) RT-PCR analysis of FABP5 and enolase 1. (E) Western blot analysis of HSP27.

These results were selectively confirmed with immunoblotting and immunofluorescence, showing the reliability of the 2-D DIGE analysis. To the best of our knowledge, this is the first report in which proteomic dynamic changes during the catagen development have been investigated using 2-D DIGE technology.

The catagen phase is a highly controlled process of coordinated cell differentiation and apoptosis [7]. The altered expression of keratins in *Smad4* mutants revealed by this study indicated that the loss of Smad4-mediated TGF-β resulted in abnormal differentiation of keratinocytes during the HF cycling. Keratins are a family of proteins forming the intermediate filaments of epithelia that are expressed in a cell type- and differentiation-specific manner. HFs have a more complex expression pattern of keratins [24]. In the present study, the expression of keratins 5 and 14, markers of the basal layer of the epidermis and the ORS of HFs, and keratins 1 and 10, markers of the differentiating suprabasal epidermis and the IRS of HFs [24], were significantly higher in *Smad4*$^{-/-}$ mice at P20 than in *Smad4*$^{+/+}$ control mice. These findings were consistent with data from previous studies that revealed that *Smad4* mutant HFs resisted to regression and were still in an anagen-like state at P20 [14]. Consequently, the *Smad4* mutant epidermis and the HF ORS were abnormally thickened. Keratin 15 is a well-established marker of HF stem cells that reside in a special niche

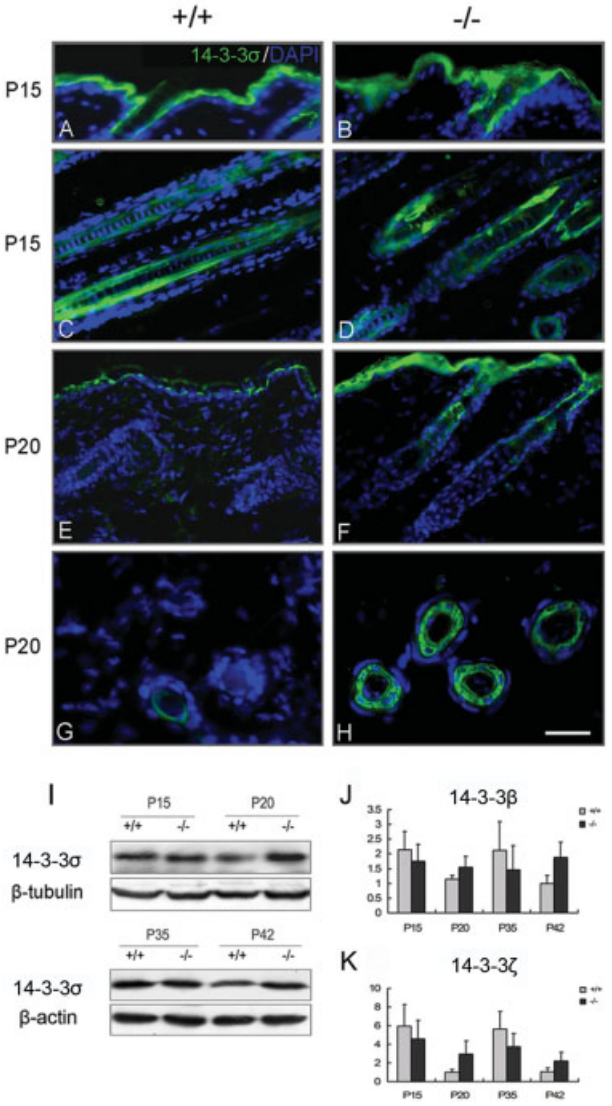

Figure 5. The deregulation of 14-3-3 proteins in *Smad4* mutants during the HF cycling. Immunofluorescence staining of 14-3-3σ performed on *Smad4*$^{+/+}$ (A, C, E, and G) and *Smad4*$^{-/-}$ (B, D, F, and H) skin sections showed that 14-3-3σ was down-regulated in P20 *Smad4*$^{+/+}$ epidermis (E) and ORS of HFs (G), but not in P20 *Smad4* mutants. (I) Western blot analysis of 14-3-3σ during the first and second hair follicle cyclings. (J, K) qRT-PCR analysis of 14-3-3β (J) and 14-3-3ζ (K). Scale bar: (A, B, G, and H) 14 μm; (C, D, E, and F) 20 μm.

at the bulge. It is also expressed in the basal keratinocytes of stratified tissues [25, 26]. Interestingly, unlike most of the keratins which were up-regulated in *Smad4* mutants, keratin 15 was significantly down-regulated. Previous studies have reported that keratin 15 is not compatible with keratinocyte activation and is down-regulated in order to maintain the activated phenotype [26]. The decreased expression of keratin 15 in this study demonstrated that *Smad4* deficient keratinocytes were persistently activated. This is largely consistent with our previous findings that reported an increased number of proliferating cells in the *Smad4*$^{-/-}$ epidermis and HFs at P20 than in controls [14].

In addition to keratins, we also identified a number of proteins known to regulate cell proliferation, differentiation, and apoptosis, such as cathepsin D and HSP27, were differentially expressed between the epidermis of *Smad4*$^{+/+}$ and *Smad4*$^{-/-}$ mice. A couple of previous studies have implicated that cathepsin D and HSP27 could be directly regulated by TGF-β [27, 28]. Two isoforms of cathepsin D were differentially expressed in response to activation of TGF-β receptors in MCF10A mammary epithelial cells overexpressing the HER2/Neu (ErbB2) oncogene [27]. It has also been reported that the TGF-β1-induced cell invasion is mediated through activation of HSP27 [28]. Consistently, we found the decreased expression of HSP27 in *Smad4* mutant epidermis at both P15 and P20.

Notably, we showed that 14-3-3σ together with other 14-3-3 proteins were differentially expressed between P15 and P20 in the wild-type epidermis. Furthermore, they failed to be down-regulated in the *Smad4* mutant epidermis at P20. These findings indicated that the aberrant expression of 14-3-3 proteins might contribute to the *Smad4* mutant phenotype. Previous studies have demonstrated that 14-3-3σ is a crucial regulator for keratinocyte proliferation, differentiation, and migration [29–32]. In addition, 14-3-3σ is a negative regulator of the cell cycle since it induces a G2/M arrest [33]. Studies of human keratinocytes have shown that 14-3-3σ expression is induced during the exit of keratinocytes from the stem cell compartment [34]. The depletion of 14-3-3σ in primary human keratinocytes result in the continuous proliferation and immortalization of keratinocytes [35]. Proteomic studies have revealed down-regulation of 14-3-3σ in invasive bladder transitional cell carcinomas [36]. A mutation in 14-3-3σ is responsible for the repeated epilation phenotype in mice [31, 37]. Recent works have demonstrated that 14-3-3σ could interact with interferon regulatory factor 6 and keratin 17 to regulate keratinocyte proliferation and differentiation [30, 32]. Here, we show for the first time, that the expression of 14-3-3σ was temporally regulated during the HF cycling, suggesting a pivotal role of 14-3-3σ in controlling catagen initiation.

Keratinocyte apoptosis is a central element in the regulation of HF regression [3]. Apoptosis during catagen development correlates largely with a down-regulation of the Bcl-2/Bax ratio [3]. Previous studies have shown that 14-3-3σ regulates apoptosis through its interactions with the two proapoptotic proteins, Bax, and Bad [38]. 14-3-3σ and 14-3-3θ interact with Bax in a phosphorylation-independent manner, leading to the sequestration of Bax in the cytoplasm, thus preventing the cell from entering apoptosis [10, 39]. On the other hand, 14-3-3 interacts with Bad, resulting in its dissociation from Bcl2 or Bclx and blockade of the proapoptotic effects of Bad [40]. Recently, similar effects upon interaction of 14-3-3ζ with AKT-specific phospho-Bad have been reported [41]. A recent study reported that Smad proteins could

enhance 3-phosphoinositide-dependent protein kinase-1 (PDK1) activity and Bad phosphorylation by removing 14-3-3, a negative regulator of PDK1, from the PDK1-14-3-3 complex [42]. In this study, we reveal that the increased 14-3-3 proteins might be responsible for the blockade of catagen initiation in *Smad4* deficient mice, suggesting that TGF-β signaling could induce catagen by down-regulating 14-3-3 proteins. This needs to be further clarified.

In conclusion, by identifying proteomic dynamic protein changes during the catagen development in *Smad4* mutant and control mice, the 2-D DIGE proteomics approach has given significant new insights into the function of epidermal Smad4-mediated TGF-β signals in controlling the initiation of catagen.

We thank Chuxia Deng (NIH, USA) for Smad4 floxed mouse. This work was supported by the National Key Basic Research Program of China (2005CB522506; 2007CB91H100; 2007CB71H104), Hi-Tech R&D Program (2006AA02Z168) and National Science Supporting Program (2006BAI23B01-3), National Natural Science Foundation of China (30430350; 20735005; 20505019; 20635010), Beijing Science Projects (Z0006303041231).

The authors have declared no conflict of interest.

5 References

[1] Stenn, K. S., Paus, R., Controls of hair follicle cycling. *Physiol. Rev.* 2001, *81*, 449–494.

[2] Lindner, G., Botchkarev, V. A., Botchkareva N. V., Ling G. *et al.* Analysis of apoptosis during hair follicle regression (catagen). *Am. J. Pathol.* 1997, *151*, 1601–1617.

[3] Botchkareva, N. V., Ahluwalia, G., Shander, D., Apoptosis in the hair follicle. *J. Invest. Dermatol.* 2006, *126*, 258–264.

[4] Mazzieri, R., Jurukovski, V., Obata, H., Sung, J. *et al.*, Expression of truncated latent TGF-beta-binding protein modulates TGF-beta signaling. *J. Cell Sci.* 2005, *118*, 2177–2187.

[5] Foitzik, K., Lindner, G., Mueller-Roever, S., Maurer, M. *et al.*, Control of murine hair follicle regression (catagen) by TGF-beta1 in vivo. *FASEB J.* 2000, *14*, 752–760.

[6] Soma, T., Hibino, T., Dominant Bcl-2 expression during telogen-anagen transition phase in human hair. *J. Dermatol. Sci.* 2004, *36*, 183–185.

[7] Botchkarev, V. A., Botchkareva, N. V., Roth, W., Nakamura, M. *et al.*, Noggin is a mesenchymally derived stimulator of hair-follicle induction. *Nat. Cell Biol.* 1999, *1*, 158–164.

[8] Foitzik, K., Spexard, T., Nakamura, M. Halsner, U., Paus, R., Towards dissecting the pathogenesis of retinoid-induced hair loss: All-trans retinoic acid induces premature hair follicle regression (catagen) by upregulation of transforming growth factor-beta2 in the dermal papilla. *J. Invest. Dermatol.* 2005, *124*, 1119–1126.

[9] Soma, T., Tsuji, Y., Hibino, T., Involvement of transforming growth factor-beta2 in catagen induction during the human hair cycle. *J. Invest. Dermatol.* 2002, *118*, 993–997.

[10] Nomura, M., Shimizu, S., Sugiyama, T., Narita, M. *et al.*, 14-3-3 Interacts directly with and negatively regulates pro-apoptotic Bax. *J. Biol. Chem.* 2003, *278*, 2058–2065.

[11] Nakamura, M., Matzuk, M. M., Gerstmayer, B., Bosio, A. *et al.*, Control of pelage hair follicle development and cycling by complex interactions between follistatin and activin. *FASEB J.* 2003, *17*, 497–499.

[12] Shi, Y., Massague, J., Mechanisms of TGF-beta signaling from cell membrane to the nucleus. *Cell* 2003, *113*, 685–700.

[13] Blain, S. W., Massague, J., Different sensitivity of the transforming growth factor-beta cell cycle arrest pathway to c-Myc and MDM-2. *J. Biol. Chem.* 2000, *275*, 32066–32070.

[14] Ito, M., Liu, Y., Yang, Z., Nguyen, J. *et al.*, Stem cells in the hair follicle bulge contribute to wound repair but not to homeostasis of the epidermis. *Nat. Med.* 2005, *11*, 1351–1354.

[15] Qiao, W., Li, A. G., Owens, P., Xu, X. *et al.*, Hair follicle defects and squamous cell carcinoma formation in Smad4 conditional knockout mouse skin. *Oncogene* 2006, *25*, 207–217.

[16] Mao, C. M., Yang, X., Cheng, X., Lv, Y. X. *et al.*, Establishment of keratinocyte-specific Cre recombinase transgenic mice. *Yi Chuan Xue Bao* 2003, *30*, 407–413.

[17] Yang, X., Li, C., Herrera, P. L., Deng, C. X., Generation of Smad4/Dpc4 conditional knockout mice. *Genesis* 2002, *32*, 80–81.

[18] Teng, Y., Sun, A. N., Pan, X. C., Yang, G. *et al.*, Synergistic function of Smad4 and PTEN in suppressing forestomach squamous cell carcinoma in the mouse. *Cancer Res.* 2006, *66*, 6972–6981.

[19] Huang, C. M., Foster, K. W., DeSilva, T., Zhang, J. *et al.*, Comparative proteomic profiling of murine skin. *J. Invest. Dermatol.* 2003, *121*, 51–64.

[20] Wang, Y., Zhang, Y., Zeng, Y., Zheng, Y. *et al.*, Patterns of nestin expression in human skin. *Cell Biol. Int.* 2006, *30*, 144–148.

[21] Hogewoning, A. A., Boxman, I. L., Condylomata acuminata: A rare symptom of ubiquitous human papillomavirus and not a sign of risky sex behavior. *Ned. Tijdschr. Geneeskd.* 1999, *143*, 2491.

[22] Gu, L. H., Coulombe, P. A., Keratin function in skin epithelia: A broadening palette with surprising shades. *Curr. Opin. Cell Biol.* 2007, *19*, 13–23.

[23] Molloy, M. P., Brzezinski, E. E., Hang, J., McDowell, M. T., VanBogelen, R. A., Overcoming technical variation and biological variation in quantitative proteomics. *Proteomics* 2003, *3*, 1912–1919.

[24] Smith, F., The molecular genetics of keratin disorders. *Am. J. Clin. Dermatol.* 2003, *4*, 347–364.

[25] Lyle, S., Christofidou-Solomidou, M., Liu, Y., Elder, D. E. *et al.*, The C8/144B monoclonal antibody recognizes cytokeratin 15 and defines the location of human hair follicle stem cells. *J. Cell Sci.* 1998, *111*, 3179–3188.

[26] Waseem, A., Dogan, B., Tidman, N., Alam, Y. *et al.*, Keratin 15 expression in stratified epithelia: Downregulation in activated keratinocytes. *J. Invest. Dermatol.* 1999, *112*, 362–369.

[27] Friedman, D. B., Wang, S. E., Whitwell, C. W., Caprioli, R. M. *et al.*, Multivariable difference gel electrophoresis and mass

spectrometry: A case study on transforming growth factor-beta and ERBB2 signaling. *Mol. Cell. Proteomics* 2007, *6*, 150–169.

[28] Xu, L., Chen, S., Bergan, R. C., MAPKAPK2 and HSP27 are downstream effectors of p38 MAP kinase-mediated matrix metalloproteinase type 2 activation and cell invasion in human prostate cancer. *Oncogene* 2006, *25*, 2987–2998.

[29] Santoro, M. M., Gaudino, G., Marchisio, P. C., The MSP receptor regulates alpha6beta4 and alpha3beta1 integrins via 14-3-3 proteins in keratinocyte migration. *Dev. Cell* 2003, *5*, 257–271.

[30] Murayama, K., Kimura, T., Tarutani, M., Tomooka, M. *et al.*, Akt activation induces epidermal hyperplasia and proliferation of epidermal progenitors. *Oncogene* 2007, *26*, 4882–4888.

[31] Li, Q., Lu, Q., Estepa, G., Verma, L. M., Identification of 14-3-3sigma mutation causing cutaneous abnormality in repeated-epilation mutant mouse. *Proc. Natl. Acad. Sci. USA* 2005, *102*, 15977–15982.

[32] Richardson, R. J., Dixon, J., Malhotra, S., Hardman, M. J. *et al.*, Irf6 is a key determinant of the keratinocyte proliferation-differentiation switch. *Nat. Genet.* 2006, *38*, 1329–1334.

[33] He, T. C., Sparks, A. B., Rago, C., Hermeking, H. *et al.*, Identification of c-MYC as a target of the APC pathway. *Science* 1998, *281*, 1509–1512.

[34] Torok, L., Gurbity, P. T., Kirschner, A., Krenacs, L., Panniculitis-like lymphoma clinically manifesting as alopecia. *Orv. Hetil.* 2002, *143*, 607–609.

[35] Dellambra, E., Golisano, O., Bondanza, S., Siviero, E. *et al.*, Downregulation of 14-3-3sigma prevents clonal evolution and leads to immortalization of primary human keratinocytes. *J. Cell Biol.* 2000, *149*, 1117–1130.

[36] Moreira, J. M., Gromov, P., Celis, J. E., Expression of the tumor suppressor protein 14-3-3 sigma is down-regulated in invasive transitional cell carcinomas of the urinary bladder undergoing epithelial-to-mesenchymal transition. *Mol. Cell. Proteomics* 2004, *3*, 410–419.

[37] Chang, E., Yang, J., Nagavarapu, U., Herron, G. S., Aging and survival of cutaneous microvasculature. *J. Invest. Dermatol.* 2002, *118*, 752–758.

[38] Mhawech, P., 14-3-3 proteins–an update. *Cell Res.* 2005, *15*, 228–236.

[39] Reep, R. L., Stoll, M. L., Marshall, C. D., Homer, B. L., Samuelson, D. A., Microanatomy of facial vibrissae in the Florida manatee: The basis for specialized sensory function and oripulation. *Brain Behav. Evol.* 2001, *58*, 1–14.

[40] Tani, H., Morris, R. J., Kaur, P., Enrichment for murine keratinocyte stem cells based on cell surface phenotype. *Proc. Natl. Acad. Sci. USA* 2000, *97*, 10960–10965.

[41] Claerhout, S., Decraene, D., Van Laethem, A., Van Kelst, S. *et al.*, AKT delays the early-activated apoptotic pathway in UVB-irradiated keratinocytes via BAD translocation. *J. Invest. Dermatol.* 2007, *127*, 429–438.

[42] Seong, H. A., Jung, H., Kim, K. T., Ha, H., 3-Phosphoinositide-dependent PDK1 negatively regulates transforming growth factor-beta-induced signaling in a kinase-dependent manner through physical interaction with Smad proteins. *J. Biol. Chem.* 2007, *282*, 12272–12289.

